

Biology Contribution

Focused Ultrasound-Mediated Blood-Brain Barrier Opening Increases Delivery and Efficacy of Etoposide for Glioblastoma Treatment

Hong-Jian Wei, PhD,^{*} Pavan S. Upadhyayula, BS,[†]
 Antonios N. Pouliopoulos, PhD,[‡] Zachary K. Englander, MD, MS,[†]
 Xu Zhang, PhD,^{§,||} Chia-Ing Jan, MD, PhD,^{¶,#,*,††} Jia Guo, PhD,^{‡‡}
 Angeliki Mela, PhD,[¶] Zhiguo Zhang, PhD,^{§,||} Tony J.C. Wang, MD,^{*,†,§§}
 Jeffrey N. Bruce, MD,^{†,§§} Peter D. Canoll, MD, PhD,^{¶,§§}
 Neil A. Feldstein, MD,[†] Stergios Zacharoulis, MD,^{||}
 Elisa E. Konofagou, PhD,[‡] and Cheng-Chia Wu, MD, PhD^{*,§§}

**Department of Radiation Oncology, Columbia University Irving Medical Center, New York, New York; †Department of Neurological Surgery, Columbia University Irving Medical Center, New York, New York; ‡Department of Biomedical Engineering, Columbia University, New York, New York; §Institute for Cancer Genetics, Columbia University Irving Medical Center, New York, New York; ||Department of Pediatrics, Columbia University Irving Medical Center, New York, New York; ¶Department of Pathology and Cell Biology, Columbia University Irving Medical Center, New York, New York; #Division of Molecular Pathology, Department of Pathology, China Medical University and Hospital, Taichung, Taiwan; **Department of Medicine, China Medical University, Taichung, Taiwan; ††Translational Cell Therapy Center, Department of Medical Research, China Medical University Hospital, Taichung, Taiwan; ‡‡Department of Psychiatry, Columbia University, New York, New York; and §§Herbert Irving Comprehensive Cancer Center, New York, New York*

Received Jun 23, 2020. Accepted for publication Dec 13, 2020.

Corresponding author: Cheng-Chia Wu, MD, PhD; E-mail: cw2666@cumc.columbia.edu

This research was funded by the Gary and Yael Fegel Family Foundation, the Star and Storm Foundation, the Matheson Foundation (UR010590), a Herbert Irving Cancer Center Cancer Center Support Grant (P30CA013696), a Herbert Irving Cancer Center Cancer Center CAPRI Grant (NIH R38CA231577-01), National Institutes of Health (NIH) grants (5R01EB009041, 5R01AG038961, 5P01CA207206-04, and R01CA204297), and the National Center for Advancing Translational Sciences, NIH (UL1TR001873). The content is solely the responsibility of the authors and does not necessarily represent the official views of the NIH.

Disclosures: T.J.C.W. reports personal fees and non-financial support from AbbVie, personal fees from AstraZeneca, personal fees from Cancer Panels, personal fees from Doximity, personal fees and non-financial

support from Elekta, personal fees and non-financial support from Merck, personal fees and non-financial support from Novocure, personal fees and non-financial support from RTOG Foundation, personal fees from Rutgers, personal fees from University of Iowa, personal fees from Wolters Kluwer, grants and non-financial support from Genentech, outside the submitted work.

Research data are included in this published article and its supplementary information files.

Supplementary material for this article can be found at <https://doi.org/10.1016/j.ijrobp.2020.12.019>.

Acknowledgments—The authors acknowledge Maggie and Jacob Dyson and the Zuckerman Mind Brain Behavior Institute MRI Platform, a shared resource.

Purpose: Glioblastoma (GBM) is a devastating disease. With the current treatment of surgery followed by chemoradiation, outcomes remain poor, with median survival of only 15 months and a 5-year survival rate of 6.8%. A challenge in treating GBM is the heterogeneous integrity of the blood-brain barrier (BBB), which limits the bioavailability of systemic therapies to the brain. There is a growing interest in enhancing drug delivery by opening the BBB with the use of focused ultrasound (FUS). We hypothesize that an FUS-mediated BBB opening can enhance the delivery of etoposide for a therapeutic benefit in GBM.

Methods and Materials: A murine glioma cell line (Pdgf⁺, Pten^{-/-}, P53^{-/-}) was orthotopically injected into B6(Cg)-Tyrc-2/J mice to establish the syngeneic GBM model for this study. Animals were treated with FUS and microbubbles to open the BBB to enhance the delivery of systemic etoposide. Magnetic resonance (MR) imaging was used to evaluate the BBB opening and tumor progression. Liquid chromatography tandem mass spectrometry was used to measure etoposide concentrations in the intracranial tumors.

Results: The murine glioma cell line is sensitive to etoposide *in vitro*. MR imaging and passive cavitation detection demonstrate the safe and successful BBB opening with FUS. The combined treatment of an FUS-mediated BBB opening and etoposide decreased tumor growth by 45% and prolonged median overall survival by 6 days: an approximately 30% increase. The FUS-mediated BBB opening increased the brain tumor-to-serum ratio of etoposide by 3.5-fold and increased the etoposide concentration in brain tumor tissue by 8-fold compared with treatment without ultrasound.

Conclusions: The current study demonstrates that BBB opening with FUS increases intratumoral delivery of etoposide in the brain, resulting in local control and overall survival benefits. © 2020 Elsevier Inc. All rights reserved.

Introduction

Radiation therapy is an integral part of cancer treatment. More than half of patients with cancer receive radiation therapy, and the treatment paradigm ranges from definitive radiation therapy, postoperative treatment, and neoadjuvant treatment to palliative treatment.¹ In addition to traditional radiation therapy, acoustic radiation also offers a wide array of treatment options to patients with cancer. Ablative high-intensity focused ultrasound (FUS) has been used in the treatment of metastatic bone disease and prostate cancer.^{2,3} Recently, there has been a growing interest in using low-intensity FUS to open the blood-brain barrier (BBB) for drug delivery.

The BBB is a physiological barrier that maintains the homeostasis of the brain by protecting it from exogenous and endogenous substances, which can be potentially toxic.⁴ Extensive interest has emerged regarding the development of ways to optimize drug delivery by overcoming the BBB, including intracranial injections, hyperosmotic solutions, convection-enhanced delivery, and FUS-mediated BBB opening.⁵ FUS offers a potentially safe and noninvasive method to localize image-guided BBB opening for drug delivery. The optimization of FUS delivery with the combined use of microbubbles (MBs: ultrasound contrast agents) has been shown to achieve local and reversible BBB opening without damaging the brain parenchyma in multiple preclinical models, including in rodents and nonhuman primates.^{6,7} Several chemotherapeutic drugs for treating brain tumors have shown increased penetrance into the brain parenchyma after FUS and MBs induced BBB disruption, including temozolomide (TMZ), carboplatin, doxorubicin, paclitaxel, and cisplatin.⁸⁻¹² Over the past few years, there has been significant clinical advancement of FUS, with multiple FUS devices being

tested in the clinic for BBB opening in diseases, including Alzheimer disease, amyotrophic lateral sclerosis, and brain tumors.^{13,14,15} Given that FUS is a new technology, pre-clinical studies using known systemic therapies with FUS are needed for early clinical trial designs for patients with brain tumors.

Glioblastoma (GBM) is a deadly primary brain tumor in which outcomes are poor. In 2005, Stupp et al¹⁶ demonstrated a modest but significant survival benefit for GBM patients, which has become the backbone of the standard-of-care treatment for GBM for the past 15 years. Patients who undergo surgery followed by chemoradiation with TMZ have a median survival of 14.6 months, although almost every patient eventually succumbs to recurrence and their survival rarely exceeds 2 years.¹⁶ Since then, there has been minimal improvement with systemic therapy. GBM is still an incurable tumor with a median survival of 15 months and a 5-year survival rate of 6.8%.^{17,18} Despite important advances in our understanding of GBM, current systemic therapies in the clinical treatment of patients with GBM remain largely ineffective. The BBB is among the major limiting factors of systemic treatment in the clinic for GBM. GBM tumors have heterogeneous integrity of the BBB. This includes the invasive mass destroying the BBB and the diffusely infiltrative components hiding in areas of the brain where the BBB remains relatively intact. Microscopic spread is well documented from biopsy studies, demonstrating that GBM tumor cells infiltrate into adjacent edematous areas of the brain that are impermeable to contrast agents and even infiltrate up to 1 to 2 cm beyond the visible tumor.¹⁹ Typically, the destructive mass is surgically resected, while surrounding microscopic disease is targeted using adjuvant chemoradiation-based treatment. Because the penetration of systemic agents into the brain is largely restricted by the BBB, adequate treatment of the microscopic spread, which

contains intact portions of the BBB, is critical to develop an effective systemic therapy for GBM.²⁰

Etoposide is an anticancer chemotherapy drug that inhibits topoisomerase II and induces DNA strand breaks; it is widely used in the treatment of various types of cancers.²¹ Many *in vitro* and preclinical studies have shown the antitumor effects of etoposide against GBM cells.²² However, several combination therapy clinical trials with systemically delivered etoposide have shown limited antitumor activity and poor response rates, possibly due to poor BBB penetration and dose-limiting toxicities.²³⁻²⁶ Although the molecular size of etoposide is small (588.56 Da), approximately 90% of etoposide found in the body is protein bound, which may limit its bioavailability in tumors in the brain.²⁷ Thus, we hypothesize that in the setting of subtherapeutic levels of intratumoral etoposide, the addition of FUS-mediated BBB opening can enhance delivery and efficacy in treating GBM. The aim of this study is to investigate the effects of FUS-enhanced etoposide delivery on local tumor growth and overall survival.

Methods and Materials

Cell culture

The murine glioma cell line is established from the tumor generated by injecting PDGF-IRES-Cre retrovirus into the subcortical white matter of mice with floxed *Pten* and *p53*.²⁸ The murine glioma cell harboring *Pdgf*⁺, *Pten*^{-/-}, and *P53*^{-/-} (MGPP3) is cultured in DMEM medium supplemented with 0.5% fetal bovine serum, 100 units/mL penicillin, 100 µg/mL streptomycin, 0.25 µg/mL amphotericin B, 1% N2 supplement, and 10 ng/mL recombinant human PDGF-AA and FGF-basic in a humidified atmosphere with 5% CO₂ at 37°C.

Cell viability assay

MGPP3 cells were seeded at a density of 7000 cells per well in a 96-well plate. After overnight culture, cells were treated with different drugs as indicated. The concentration ranges of each drug are 0.001 to 30 µM for etoposide, 0.01 to 100 µM for carboplatin, and 0.01 to 1000 µM for TMZ. After 72 hours of treatment, later cell viability was determined by the CellTiter-Blue Cell Viability Assay (Promega, Madison, WI) according to the manufacturer's instructions.

Animal studies

All animal studies were approved by the Institutional Animal Care and Use Committee of Columbia University. We purchased 4- to 6-week-old male B6(Cg)-Tyr²J/J mice from the Jackson Laboratory (Bar Harbor, ME). The mice were housed under pathogen-free conditions and fed autoclaved food and water. All animals were monitored daily for food and water intake and nutritional status (weekly

weight), and animal behaviors were assessed routinely and consistently. For etoposide administration, mice were injected intraperitoneally immediately after FUS application. For survival study, tumor-bearing mice were inspected and weighed daily. The endpoints of the survival curve were weight loss >20%; hunched posture; lethargy; persistent recumbency; coughing; labored breathing; rough hair coats; nasal discharge; jaundice; neurologic signs (circling, head pressing, seizures); bleeding from any orifice; self-induced trauma; any condition interfering with eating or drinking, such as difficulty ambulating; and death.

Intracranial injection

Mice were anesthetized by intraperitoneal injection of 100 mg/kg body weight (bw) ketamine and 10 mg/kg bw xylazine. Mice were then immobilized in a mouse stereotaxic instrument (Stoelting, Wood Dale, IL), and a 1-cm incision was made in the midline of the scalp to expose the sagittal suture and bregma of the skull. A burr hole of 1 mm in diameter was made at a position of 2 mm anterior and 2 mm lateral right to the bregma. A Hamilton syringe containing MGPP3 cells was inserted 2 mm deep from the skull surface. We injected 50,000 cells in 1 µL DMEM medium at 0.2 µL/min into the brains.

Magnetic resonance imaging

Bruker BioSpec 9.4T Magnetic Resonance Imager and ParaVision 6.0.1 (Bruker, Billerica, MA) were used for the magnetic resonance imaging. Mice were first anesthetized with 1% to 2% isoflurane, and their vital signs were monitored throughout the imaging sessions. We then placed the anesthetized mice in a phased-array radiofrequency coil. A T1-weighted 2D fast low-angle shot sequence (repetition time (TR)/echo time (TE), 230/3.3 ms; flip angle, 70°; number of excitations, 4; field of view, 25.6 mm × 25.6 mm; resolution, 100 µm × 100 µm × 400 µm) was performed 10 min after intraperitoneal injection of 0.2 mL gadodiamide (Omniscan, GE Healthcare, Chicago, IL). The tumor volumes of magnetic resonance (MR) images were quantitated using the free, open-source platform 3-dimensional Slicer (www.slicer.org). Briefly, the tumor boundaries of each consecutive slice containing tumor were contoured, and then the calculation of whole tumor volumes was conducted. Image processing methods for quantifying the BBB opening volume and contrast enhancement were as described previously.²⁹

FUS and passive cavitation detection

The experimental setup is shown in [Figure E1](#). A single-element, spherical FUS transducer (center frequency, 1.5 MHz; focal length, 60 mm; diameter, 60 mm; Imasonic) was driven by a function generator (33500B Series, Agilent Technologies, Santa Clara, CA) through a 50 dB power

amplifier (E&I Inc, Rochester, NY). A single-element, pulse-echo transducer (frequency, 7.5 MHz; focal length, 60 mm; diameter, 11.2 mm; Olympus NDT, Waltham, MA) used for passive cavitation detection (PCD) was concentrically aligned with the FUS transducer. The PCD transducer connected to a digitizer (Gage Applied Technologies, Inc, Lachine, Canada) and was used to passively acquire acoustic emissions from MBs during the FUS exposure. A cone filled with degassed, distilled water was mounted onto the transducer assembly. The transducers were attached to a computer-controlled 3-dimensional positioning system (Velmex Inc, Lachine, Canada). The polydisperse in-house manufactured MBs (concentration, 8×10^8 bubbles/mL; diameter, $1.37 \pm 1.02 \mu\text{m}$ ³⁰; lipid shell composition, DSPC and DSPE-PEG2000 at a molar ratio of 9:1; gas core, C4F10; dose, 1 $\mu\text{L/g}$ bw) were diluted in saline to 200 μL and injected intravenously. Before administration of the MBs, a 2-second sonication was applied to get the baseline of the acoustic response used in the quantification of the cavitation dose. To completely cover the tumor and its surrounding infiltrative region, FUS was applied once at each of 4 points on a 1.5 mm \times 1.5 mm grid. One hundred microliters of MBs were slowly injected before the first and third points of sonication. Each point was sonicated for 30 seconds, with a pulse repetition frequency of 5 Hz, a pulse length of 1 ms, and an estimated derated peak-negative acoustic pressure of 0.7 MPa. Acoustic emissions were recorded passively by the imaging transducer and analyzed as previously described.³¹ The acoustic energy emitted by MBs was measured over the duration of the whole sonication. Moreover, we conducted a frequency analysis using a fast Fourier Transform in MATLAB (The MathWorks, Natick, MA) to identify the MB response based on spectral features. Lastly, we calculated cavitation doses, including stable cavitation doses based on harmonics (SCDh), stable cavitation doses based on ultraharmonics (SCDu), and inertial cavitation doses (ICD) as previously described.³²

Histology

At 10 days after intracranial injection of MGPP3 cells, mice were anesthetized by an intraperitoneal injection of 100 mg/kg bw ketamine and 10 mg/kg bw xylazine and were then transcardially perfused with 0.9% sodium chloride solution for 10 minutes. After perfusion, brain tissues were collected, fixed in 4% paraformaldehyde, processed, and embedded in paraffin. Hematoxylin and eosin (H&E) staining was performed, and the slides were analyzed by the neuropathologists.

Liquid chromatography with tandem mass spectrometry

At 7 days after the intracranial injection of MGPP3 cells, FUS was performed on mice to open the BBB. Right after FUS application, 5 mg/kg bw of etoposide was

intraperitoneally administered. At 90 minutes after the intraperitoneal administration of etoposide, mice were anesthetized by an intraperitoneal injection of 100 mg/kg bw ketamine and 10 mg/kg bw xylazine. Blood samples were collected by cardiac puncture. We then conducted transcardial perfusion with 0.9% sodium chloride solution for 10 minutes and collected the brain tissues with the tumor. For serum collection, whole blood samples were allowed to clot for 60 minutes and then centrifuged at $2000 \times g$ for 20 minutes to acquire the supernatants (serum). All samples were stored at -80°C until analyzed by the Biomarkers Core Laboratory of the Irving Institute for Clinical and Translational Research (Columbia University, New York, NY).

Animal numbers and statistical analysis

The sizes of the sample groups used in histology, the determination of etoposide dose, and liquid chromatography tandem mass spectrometry (LC-MS-MS) are 6, 5, and 6, respectively. The sizes of the sample groups in the survival study are as indicated in Table 1. All data presented are representative of at least 3 independent experiments that yielded similar results. Statistical analyses were performed using GraphPad Prism 5.

Results

High sensitivity of mouse glioma cell line to etoposide

Initially, we examined the drug sensitivity of MGPP3 cells to etoposide, carboplatin, and TMZ. TMZ is used as part of the standard of care for patients with GBM.¹⁶ Carboplatin has previously been used in a clinical trial with FUS for recurrent GBM. Cells were treated with the chemotherapy drug for 72 hours and CellTiter-Blue Assay was performed to assess for cell viability. The values of half maximal inhibitory concentrations of etoposide, carboplatin, and TMZ for MGPP3 cells were 0.47, 85.4, and 690.2 μM , respectively, indicating that the MGPP3 cells appeared to be most sensitive to etoposide (Fig. 1).

GBM features of MGPP3-derived tumor

MGPP3 is a murine glioma cell line that was isolated from mice injected with a PDGF-internal ribosomal entry site retrovirus into the cerebral white matter of Pten^{-/-}/p53^{-/-} mice. Intracranial injection of MGPP3 cells into the cerebral white matter demonstrated highly reproducible tumors in mice, recapitulating key features of human GBM. These tumors are heterogeneous, with a solid tumor component and microscopic infiltrative disease. The gene expression profile demonstrated a high degree of similarity with proneural GBM.²⁸ Typically, in the setting of preclinical murine models for GBM, mice are treated when they have a

Table 1 Summary of animal survival analysis

| Group | Median survival, d | Change in median survival time, % | <i>P</i> value* | Mean survival, [†] d | Change in mean survival time, % | <i>P</i> value [‡] |
|---|--------------------|-----------------------------------|-----------------|-------------------------------|---------------------------------|-----------------------------|
| Control, n = 13 | 19 | 100 | .0002 | 18.85 ± 3.46 | 100 | .0002 |
| Etoposide alone, n = 13 | 19 | 100 | .0001 | 19.31 ± 2.59 | 102.44 | .0001 |
| Focused ultrasound alone, n = 7 | 19 | 100 | .0014 | 19.43 ± 3.1 | 103.08 | .0037 |
| Focused ultrasound plus etoposide, n = 11 | 25 | 131.58 | - | 24.64 ± 2.84 | 130.72 | - |

* *P* values are relative to focused ultrasound plus etoposide in a log-rank test.

[†] Values are means ± standard deviations.

[‡] *P* values are relative to focused ultrasound plus etoposide in unpaired Student *t* tests with Welch's correction.

large, destructive tumor in which the BBB is diffusely disrupted. In the clinical setting, patients with GBM undergo maximal safe resection of the primary solid tumor component, and radiation and systemic therapy are used to treat the microscopic disease extending beyond the resection margin. To model the microscopic spread where the BBB disruption was minimal, we selected to treat mice implanted with MGPP3 before the formation of a destructive tumor mass. Using T1-weighted, contrast-enhanced MR imaging, we monitored the tumor progression. At 6 days after tumor implantation, MR images showed a small tumor cavity caused by the injection, surrounded by a contrast-enhanced ring with no visible mass (Fig. 2A). Mice with this radiographic finding had over 95% tumor formation. Thus, we elected to treat our mice 1 week after tumor implantation to mimic the microscopic diseases with minor BBB disruptions. We then further used T1-weighted, contrast-enhanced and noncontrast T2 MR imaging to identify the infiltrative characteristics of MGPP3-derived tumors. Mice were scanned at Day 10 after tumor implantation, once a solid tumor was visualized. Correlating to clinical radiographic findings of GBM, T2 hyperintensity (asterisk, Fig. 2B) was visualized surrounding the region of the T1 contrast-enhancing mass (arrowhead, Fig. 2B). We also analyzed the histopathologic features of the MGPP3-derived tumor. H&E staining of the tumor at Day 10 showed pleomorphic large tumor cells with huge, bizarre

nuclei and nuclear hyperchromasia. Moreover, the tumor had infiltrative margins, mild vascular proliferation, and moderate mononuclear cell infiltration (Fig. 2C, left panel). On high magnification, large tumor cells with multinucleation, prominent nucleoli, increased mitotic figures (count 11), and anisonucleosis (Fig. 2C, right panel) were observed. Collectively, the MGPP3-derived tumor exhibited the imaging and histopathologic features of GBM, with diffusely infiltrative characteristics.

FUS-mediated BBB opening and PCD in intracranial GBM model

To cover the tumor cavity and its surrounding infiltrative region, we sonicated 4 points in a 2 × 2 square at a distance of 1.5 mm by 1.5 mm apart (Fig. 3A). During sonication, PCD was used in real time to detect the acoustic emission of MBs. After sonication, T1-weighted contrast-enhanced MR imaging was used to confirm successful BBB opening. As shown in Figure 3B, the contrast-enhancing region in T1 postcontrast MR images confirmed BBB opening in the region of the tumor cavity with additional margins within the mouse brain. Acoustic energy emitted by MBs rose at the beginning due to the first MB administration (red arrowhead, Fig. 3) and maintained the energy level during sonication. In addition to this, the 3 peaks (blue

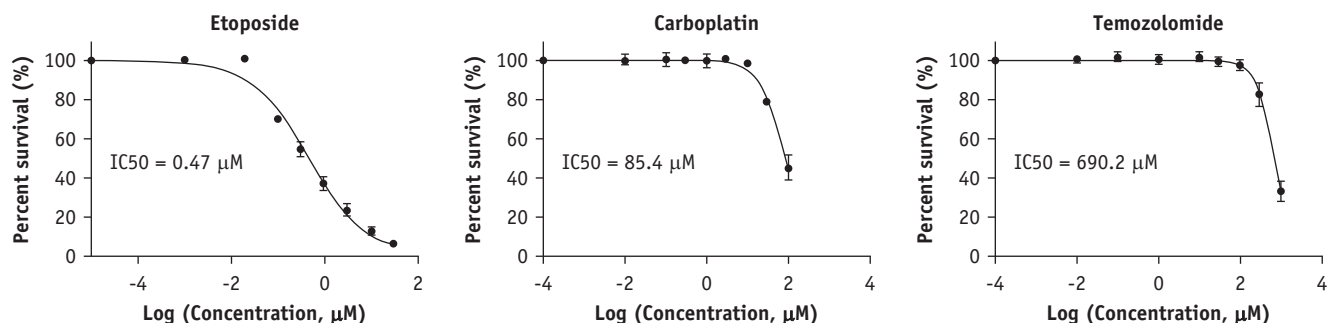


Fig. 1. In vitro cytotoxicity of chemotherapy drugs in mouse glioma cells. Cell viability (mean ± SD) of MGPP3 cells treated with etoposide, carboplatin, and TMZ for 72 hours, assessed by 3-(4,5-Dimethylthiazol-2-yl)-2,5-diphenyltetrazolium bromide (MTT) assay. *Abbreviations:* IC₅₀ = half maximal inhibitory concentration; MGPP3 = murine glioma cell harboring Pdgf⁺, Pten^{-/-}, and P53^{-/-}; SD = standard deviation; TMZ = temozolomide.

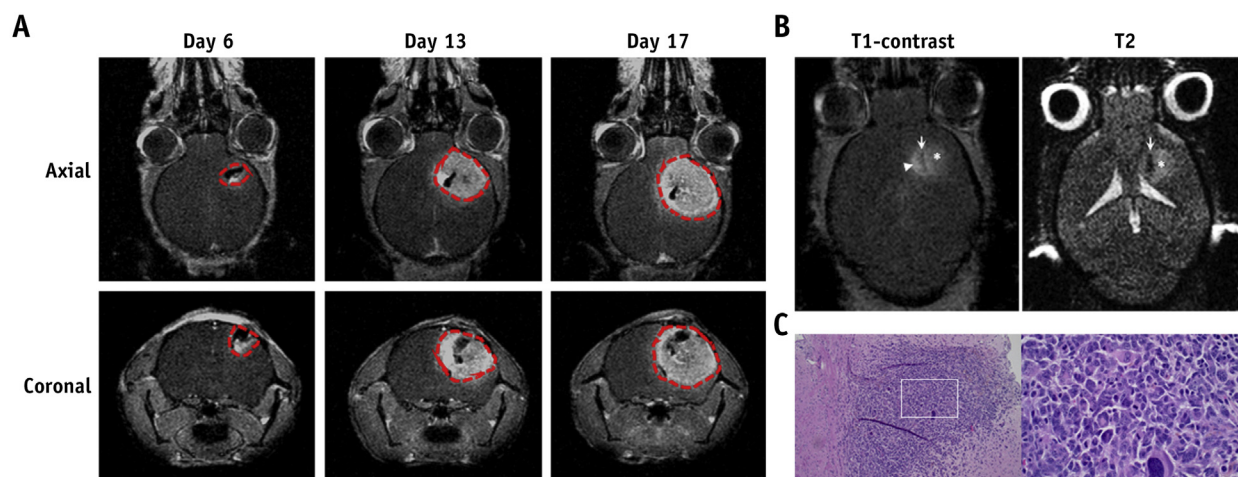


Fig. 2. Validation of intracranial GBM model. (A) Representative T1-weighted contrast-enhanced images of mice intracranially injected with MGPP3 cells. Images were taken 6, 13, and 17 days after tumor implantation. The red dotted line indicates the tumor cavity as defined by T1 postcontrast enhancement. (B) Representative T1-weighted contrast-enhanced and unenhanced T2 images of mice 10 days after intracranial injection of MGPP3 cells. The left panel shows the injection tract (arrow), contrast-enhancing tumor (arrowhead), and hyperintensity demonstrating the peritumoral edema region (asterisk). The right panel shows the injection tract (arrow) and a lightly hyperintense, poorly demarcated, and irregular tumor lesion (asterisk). (C) Representative H&E staining of a brain tumor showing the histologic features of MGPP3-derived xenograft. The left panel is shown at original magnification $\times 100$ and the right panel at original magnification $\times 400$. *Abbreviations:* GBM = glioblastoma; H&E = hematoxylin and eosin; MGPP3 = murine glioma cell harboring Pdgf^+ , $\text{Pten}^{-/}$, and $\text{P53}^{-/}$. (A color version of this figure is available at <https://doi.org/10.1016/j.ijrobp.2020.12.019>.)

arrowheads, Fig. 3) observed in the energy correspond to the motion of the transducer to another spot of the square (Fig. 3C). The spectral content of the received signals showed an increase in higher harmonics after MB

administration (Fig. 3D). A spectrogram revealed no substantial increase in the broadband floor during the FUS treatment, indicating limited microbubble destruction within the focal volume (Fig. 3E). Lastly, SCDh, SCDu,

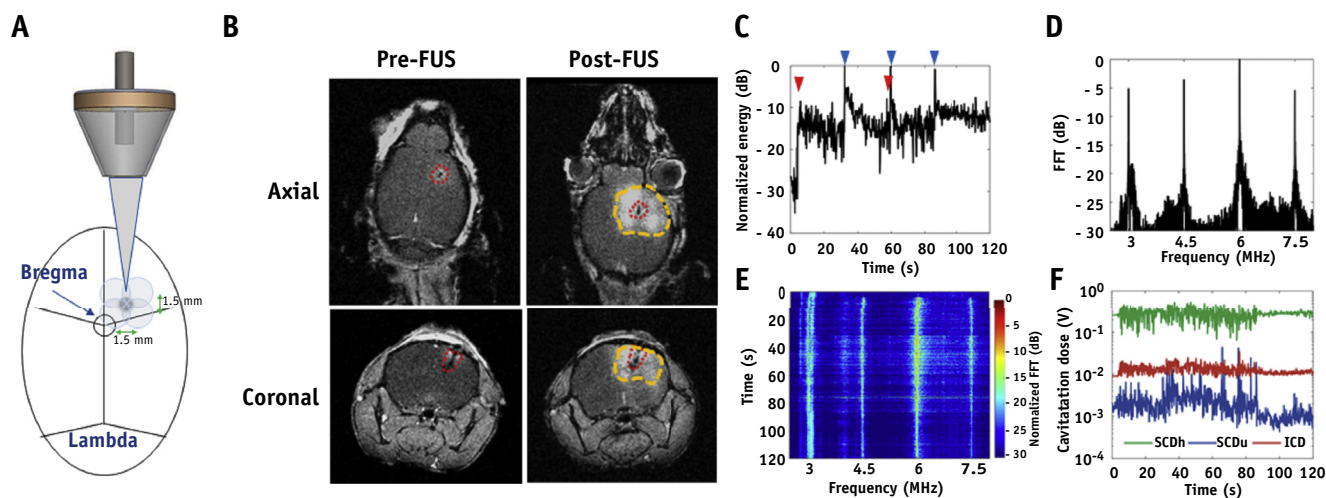


Fig. 3. FUS-mediated BBB opening confirmed by MR imaging and acoustic emissions measurement. (A) Schematic diagram of the targeted strategy for BBB opening. (B) Representative T1-weighted contrast-enhanced images of GBM tumor-bearing mice before and after FUS sonication. The red dotted line shows the tumor, and the yellow dotted line shows the BBB opening. In vivo passive cavitation detection measurements. (C) Acoustic energy, (D) spectral amplitude, and (E) spectrogram of MBs cavitation during FUS exposure. (F) The doses of SCDh, SCDu, and ICD during FUS exposure. The red arrowhead indicates MB administration, and the blue arrowheads indicate movement of the transducer. *Abbreviations:* BBB = blood-brain barrier; FFT = fast Fourier Transform; FUS = focused ultrasound; GBM = glioblastoma; ICD = inertial cavitation; MB = microbubble; MR = magnetic resonance; SCDh = stable harmonic cavitation; SCDu = stable ultra-harmonic cavitation. (A color version of this figure is available at <https://doi.org/10.1016/j.ijrobp.2020.12.019>.)

and ICD were relatively constant throughout the sonication, indicating persistent stable cavitation activity during sonication with minimal inertial cavitation (Fig. 3F).

Treatment combining FUS and etoposide reduces tumor growth and prolongs survival in an intracranial GBM model

To establish a subtherapeutic dose of etoposide without FUS in the GBM model, mice with GBM were intraperitoneally treated with 0, 5, 10, and 20 mg/kg bw of etoposide on Days 7 and 14 after tumor implantation. We found 5 mg/kg bw of etoposide was subtherapeutic (data not shown). Hence, we elected to use 5 mg/kg bw of etoposide in combination with FUS to assess whether FUS-mediated BBB opening increased etoposide delivery, resulting in an improved therapeutic benefit in GBM tumor-bearing mice. After intracranial tumor implantation, tumor-bearing mice were randomized into 4 groups: (1) controls; (2) etoposide alone; (3) FUS alone; and (4) FUS plus etoposide. The experimental timeline is shown in Figure 4A. An MR imaging T1 postcontrast scan was used to assess BBB opening and tumor size. Using MATLAB to quantify the volume of BBB opening and contrast enhancement, there was no significant difference between the FUS-alone and FUS + etoposide groups on Day 7 (BBB openings, 35.40 ± 12.59 and 29.75 ± 13.46 , respectively; contrast enhancements, 90.18 ± 31.06 and 77.75 ± 32.29 , respectively) and Day 14 (BBB openings, 30.55 ± 8.08 and 25.67 ± 10.99 , respectively; contrast enhancements, 81.24 ± 28.36 and $56.66 \pm$

20.20 , respectively; Fig. 4B and C). Likewise, quantitative results of PCD also showed similar delivery of ultrasound, achieving comparable cavitation doses across the 2 groups (Fig. 4D).

We also used T1-weighted, contrast-enhanced MR imaging to monitor tumor progression by measuring tumor volumes. Mice receiving FUS plus etoposide had increased local control compared with control mice (Fig. 5A). The animals from the control, etoposide-alone, and FUS-alone groups showed progressive tumor growth (the tumor volume changes from Day 7 to Day 14 were 5.39 ± 0.67 , 6.04 ± 1.02 , and 5.75 ± 0.45 fold, respectively). Treatment with FUS + etoposide inhibited tumor growth (tumor volume changes from Day 7 to Day 14 were 2.98 ± 0.31 fold), with a 45% reduction in tumor size compared with control mice (Fig. 5B). Kaplan-Meier survival curves showed an increase in survival in the FUS + etoposide arm (Fig. 5C; Table 1). The median survival was 19 days in the control, etoposide-alone, and FUS-alone groups. The treatment of FUS + etoposide improved the median survival of mice to 25 days. The log-rank test revealed that FUS + etoposide significantly increases median survival by 6 days, or approximately 30%, compared with other groups.

FUS-mediated BBB opening enhances etoposide delivery to brain tumor

The BBB acts as a barrier to limit large molecules from penetrating the brain parenchyma. We examined whether FUS-mediated BBB opening increased intracranial tumor

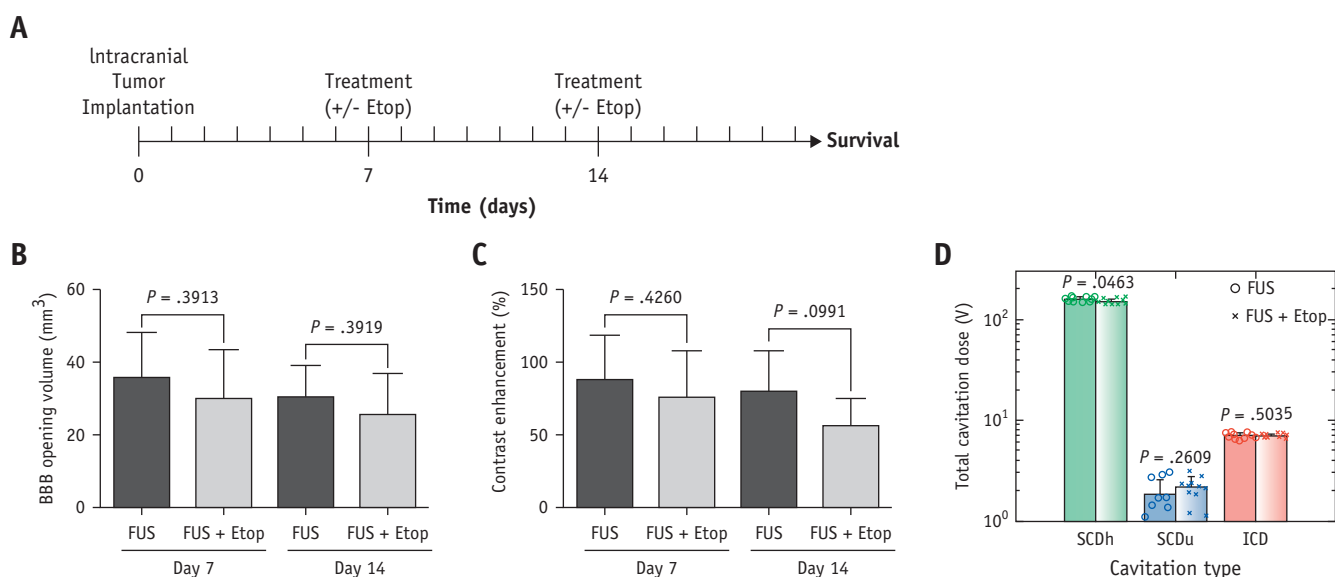


Fig. 4. Comparison of BBB opening in vivo. (A) Time course of the experiment. The quantification of MR images for (B) BBB opening volume (mm³) and (C) contrast enhancement (%). (D) Average SCDh, SCDu, and ICD doses during FUS sonication. Values are means + SD; *P* values between FUS and FUS + Etop are indicated by using unpaired *t* tests with Welch's correction. *Abbreviations:* BBB = blood-brain barrier; Etop = etoposide; FUS = focused ultrasound; ICD = inertial cavitation; MR = magnetic resonance; SCDh = stable harmonic cavitation; SCDu = stable ultraharmonic cavitation; SD = standard deviation.

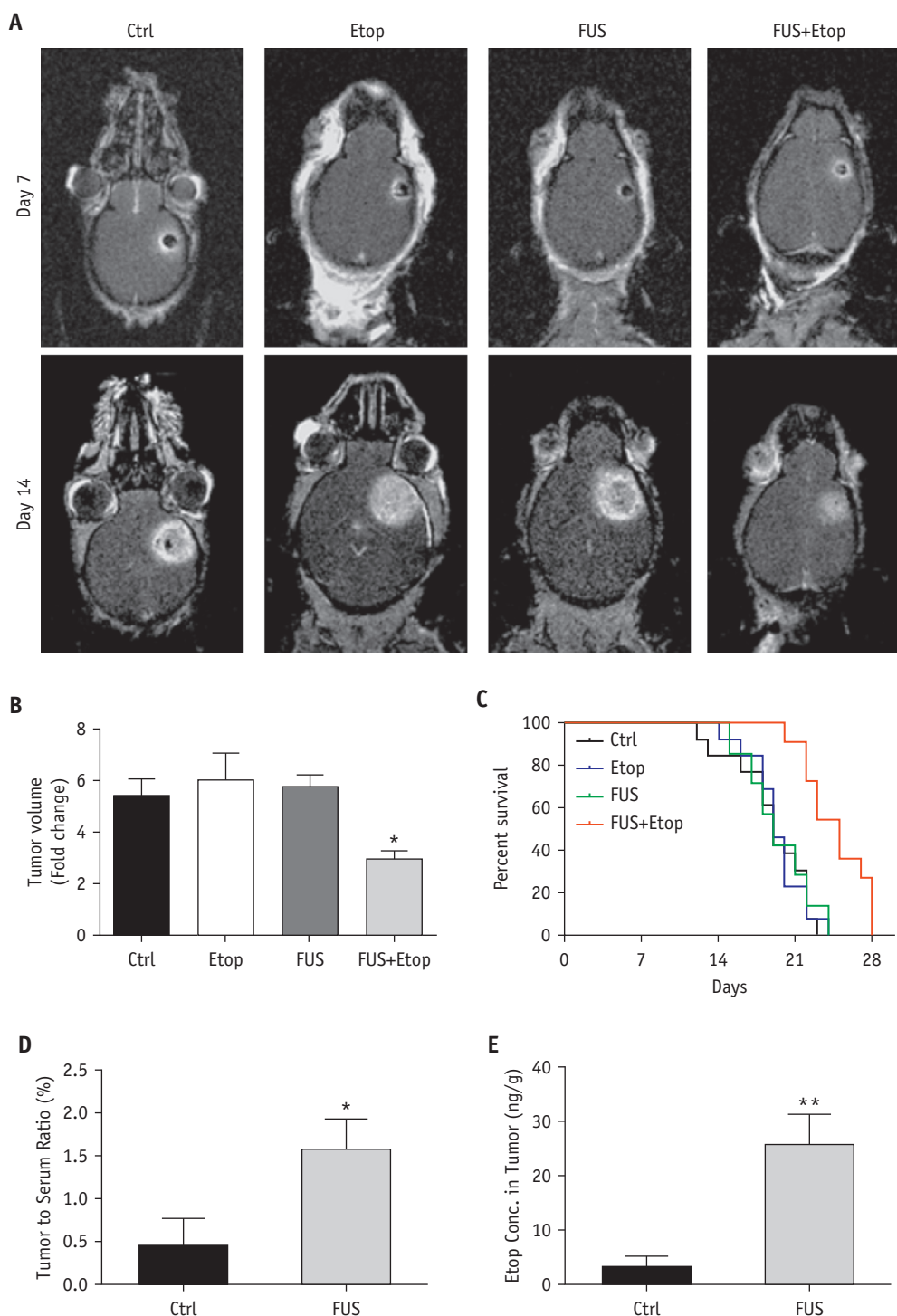


Fig. 5. Therapeutic efficacy and delivery of etoposide enhanced by FUS in GBM tumor-bearing mice. (A) Representative T1-weighted contrast-enhanced images of mice intracranially injected with MGPP3 cells with indicated treatment. Images were taken 7 and 14 days after tumor implantation. (B) Quantitative analysis of the relative tumor progression. Fold changes are the tumor volume by MR image on Day 14, normalized to the tumor volume on Day 7. Values are means + SD; * indicates a P value $< .05$ in an unpaired t test with Welch's correction, compared with the control group. (C) Kaplan-Meier plot of survival of mice intracranially injected with MGPP3 cells with indicated treatment. (D) The tumor-to-serum ratios of etoposide concentration (E) and the concentration of etoposide in brain tumors with or without FUS. *Abbreviations:* Ctrl = control group; Etop = etoposide; FUS = focused ultrasound; GBM = glioblastoma; MGPP3 = murine glioma cell harboring $Pdgf^{+}$, $Pten^{-/-}$, and $P53^{-/-}$; MR = magnetic resonance; SD = standard deviation.

delivery of etoposide. LC-MS-MS was used to measure the concentration of etoposide in the tissues and serum of GBM-harboring mice with or without FUS. At 7 days after tumor implantation, mice were exposed to FUS to open BBB and were intraperitoneally administered with 5 mg/kg bw of etoposide. The LC-MS-MS results showed that mice receiving FUS had a 3.5-fold increased mean brain tumor-to-serum ratio compared with control mice (Fig. 5D). The concentration of etoposide in the sonicated tumor tissue was over 8-fold higher than in the non-sonicated tumor tissue (Fig. 5E). These results suggest that FUS can increase the accumulation of etoposide in the tumor tissue of mouse brains.

Discussion

GBM is a devastating brain tumor for which there has been minimal clinical systemic therapeutic advancements over the past 15 years. The diffusely infiltrative nature of the disease makes it difficult to eliminate microscopic disease even after gross total resection. GBM is heterogeneous, with both a solid component (in which the BBB is disrupted) and an extensively infiltrative microscopic component that extends into regions of the brain where the BBB remains relatively intact. This is demonstrated by MR imaging, where the T1-weighted postcontrast images show contrast enhancement confined to the primary tumor mass with disrupted BBB (which is typically resected); the area of infiltrating tumor cells, visualized as hyperintense regions on T2-weighted imaging, extends beyond the primary tumor and reveals minimal contrast enhancement.³³ Radiation treatment has played a critical role in the management of this microscopic disease, with ionization radiation therapy; however, the overall survival is dismal. Over 90% of patients with GBM have recurrences within 2 to 3 cm from the margin of the original resected tumor.^{34,35} The heterogeneous integrity of the BBB in GBM plays a big role in limiting drug delivery, and novel approaches for treatment are necessary.

There is a large disconnect between clinical and preclinical GBM. Despite the triumph of systemic treatments of preclinical mouse models of GBM, there has been very limited success in the translation of these systemic therapies for patients. A potential reason is the heterogeneous nature of the tumor and peritumoral vasculature: the residual, nonenhancing disease that is not targeted with surgery remains protected from systemic therapy by the BBB. As mentioned previously, patients with GBM are treated with maximal safe resection of the bulk tumor, while systemic and radiation strategies focus on microscopic disease. This is different from preclinical models of GBM, in which many of the studies use mice with destructive solid tumors in which the BBB is completely disrupted. Furthermore, although several preclinical models of GBM have been developed, not all of them have the characteristics to recapitulate genetic, histopathologic, and biological

features of human GBM.³⁶ For example, U87 murine glioma cells used for human orthotopic modeling of GBM often form massive tumors that disrupt the BBB without microscopic infiltration.³⁷ This creates a fundamental difference in the therapeutic effects of systemic therapies and in their bioavailability.

In this study, we elected to use a murine syngeneic GBM model using MGPP3. The MGPP3 (Pdgf⁺, Pten^{-/-}, P53^{-/-}) cell line was established from genetically engineered mouse models of GBM created by injecting a PDGF-IRES-Cre retrovirus into the subcortical white matter of mice that harbor floxed tumor suppressors (PTEN and p53). Tumors from this model underwent genome-wide expression profiling with RNA sequencing and were compared with gene sets of 4 subtypes of GBM established by the Cancer Genome Atlas, revealing the highest similarity to the proneural subtype of human GBM. This murine GBM model has been identified as having genetic and histologic resemblances to human proneural GBM, and it demonstrates a modest response to radiation therapy.²⁸ Moreover, this syngeneic mouse model of GBM uses mice of C57BL/6 origin that do not require a deficient immune system, which may more closely resemble the immune response of human GBM. To mimic the microscopic disease after surgical resection seen in humans, we elected to treat the mice that were stereotactically injected with GBM cells at an earlier time point. Through serial imaging, we observed that upon developing a ring enhancement surrounding the injection cavity, over 95% of the mice developed intracranial tumors. MR imaging of tumors demonstrated T2 hyperintensity consistent with human GBM, and a pathologic analysis of H&E stains demonstrated an infiltrative pattern similar to that of clinical GBM.

Intracranial therapeutic ultrasound has gained much interest since the first MR imaging-guided FUS device for the brain was approved by the Food and Drug Administration for clinical use in 2016 for essential tremors and in 2018 for Parkinson disease. The Neuro Exablate, by Insightec, is similar to the Gamma Knife in that the ultrasound transducers are placed in a hemispherical fashion pointing to a single focus. Using MR imaging guidance, ultrasound can be delivered, leading to an increase in temperature allowing for thermal thalamotomy for patients with essential tremor and Parkinson disease.³⁸ This same device is capable of focally and transiently opening the BBB using a low-frequency ultrasound. When a low-frequency ultrasound is delivered in the presence of ultrasound contrast, or MBs, the bubbles oscillate through repeated expansion and contraction (stable cavitation). This can lead to mechanical and functional alterations of the blood vessels, resulting in temporary and reversible opening of the BBB.^{13,39} FUS has been shown to be able to transiently, repeatedly, and safely open the BBB in multiple preclinical models, including in rodents, rabbits, pigs, and nonhuman primates by optimizing acoustic parameters and MB dosages.^{6,7} Safe BBB opening has been demonstrated

in multiple phase I and phase II clinical trials in patients with Alzheimer disease, amyotrophic lateral sclerosis, and recurrent glioblastoma.⁴⁰⁻⁴³ The degree of BBB opening and the duration of BBB opening can be modified by changing the acoustic parameters and MB dosage. With excessively stronger parameters, the MBs continuously grow, resulting in a violent collapse (inertial cavitation) that leads to shock waves and turbulent flow that may result in vascular damage.³⁹ The ultrasound parameters used in this study (center frequency, 1.5 MHz; peak-negative pressure, 0.7 MPa; pulse length, 1 ms; pulse repetition frequency, 5 Hz; in-house manufactured MBs, 1 $\mu\text{L/g}$ bw) have been previously demonstrated to open the BBB without causing neural damage.⁶ Furthermore, real-time assessments of the ultrasound energy delivered along with acoustic monitoring showed evenly maintained energy levels, resulting in high levels of stable cavitation with minimal inertial cavitation. This resulted in successful and reproducible BBB opening, without compromising safety.

Several preclinical studies have shown that FUS-mediated BBB opening increased the penetrance of various systemically administered drugs, including chemotherapy drugs⁸⁻¹² and antibody-directed therapies,⁴⁴⁻⁴⁷ into the brain parenchyma, as well as into brain tumors, ranging from metastases to GBM. To support rapid translation to clinical trials, we chose a commonly used chemotherapeutic agent to combine with a novel method of drug delivery. Etoposide is a topoisomerase II inhibitor that is used in both pediatric and adult cancer patients and is well tolerated.²² The pharmacokinetics of etoposide are well understood, and the drug reaches the maximum serum concentration within a couple hours after both intravenous and oral administration.⁴⁸ Although the molecular weight is small (588.56 Da), the majority of etoposide in the body is protein bound, limiting its penetrance across the BBB. Previous studies show that local intracranial delivery of etoposide with convection-enhanced delivery improves therapeutic effects in GBM.⁴⁹ In addition, there is some clinical evidence suggesting a potential response to treatment in patients with high-grade glioma.⁵⁰ We elected to compare etoposide with carboplatin and TMZ: TMZ is used as part of the standard of care for GBM and carboplatin has been used with ultrasound-mediated BBB opening in patients with recurrent GBM, with some response. Interestingly, the IC50 showed higher levels of cell death responses with etoposide compared with either therapy, making it an ideal candidate for rapid translation into clinical trials.

Conclusion

In this study, we observed that combining FUS with etoposide increased the intratumoral delivery of etoposide, which led to a 30% increase in median overall survival. With an increased delivery of a chemotherapeutic agent into the brain with FUS, there is some concern whether this enhances toxicities. In a study by Zhang et al, the use of

different formulations of paclitaxel (albumin-bound paclitaxel and paclitaxel dissolved in cremophor) and ultrasound-guided delivery were examined. The researchers observed that paclitaxel dissolved in cremophor induced central nervous system toxicity when combined with FUS, while albumin-bound paclitaxel did not.¹² The combined usage of FUS and etoposide was well tolerated. We did not observe increased mortality or morbidity with combining FUS and etoposide, thus making etoposide an ideal agent to examine in an early phase clinical trial.

Clinical advancement of FUS technology has progressed rapidly over the past few years, with clinical trials showing safety with BBB opening in both patients with brain tumors and patients with Alzheimer's disease.⁴⁰⁻⁴² Multiple ongoing clinical trials are currently studying the safety and feasibility of BBB opening.^{14,15} SonoCloud (CarThera, France) is an implantable device fixed to the skull that delivers low-frequency (nonfocused) ultrasound for BBB opening. In addition, 3 extracranial devices are currently being tested, including the Exablate Neuro (Insightec Tirat Carmel, Israel), the NaviFUS system (NaviFUS, Taiwan), and a single-element neuronavigation-guided device developed at Columbia University. The Exablate Neuro is similar to the Gamma Knife, in which ultrasound transducers are placed in a hemispherical manner, pointing to a single focus. A stereotactic head frame is placed on the patient for radiation planning with a built-in MR imaging system. In contrast, the NaviFUS system also uses multi-channel, hemispherical, phased-array ultrasounds; however, the targeting is based on neuronavigation. Lastly, a single-element, extracranial FUS system with neuronavigation guidance has been developed at Columbia University. This neuronavigation-guided FUS system consists of a 0.25-MHz, single-element transducer coupled with real-time cavitation monitoring.³² With the advancement of ultrasound technology and the feasibility of clinical applicability, there is an emerging need for research to advance the field. We believe our study establishes a preclinical rationale to test the combination of FUS-mediated BBB opening with etoposide in patients with glioblastoma. Currently, the treatment of intracranial FUS across the world varies from radiologists, neurologists, neurosurgeons, and radiation oncologists. FUS has the potential to offer a new pathway for noninvasive drug delivery to infiltrative tumors in the brain, and researchers in the field of radiation oncology should be aware of the development of this emerging technology.

References

1. Baskar R, Lee KA, Yeo R, Yeoh KW. Cancer and radiation therapy: Current advances and future directions. *Int J Med Sci* 2012;9:193-199.
2. Napoli A, Alfieri G, Scipione R, et al. High-intensity focused ultrasound for prostate cancer. *Expert Rev Med Devices* 2020;17:427-433.
3. Bertrand AS, Iannesi A, Natale R, et al. Focused ultrasound for the treatment of bone metastases: Effectiveness and feasibility. *J Ther Ultrasound* 2018;6:8.

4. Tajes M, Ramos-Fernandez E, Weng-Jiang X, et al. The blood-brain barrier: Structure, function and therapeutic approaches to cross it. *Mol Membr Biol* 2014;31:152-167.
5. Hendricks BK, Cohen-Gadol AA, Miller JC. Novel delivery methods bypassing the blood-brain and blood-tumor barriers. *Neurosurg Focus* 2015;38:E10.
6. Konofagou EE. Optimization of the ultrasound-induced blood-brain barrier opening. *Theranostics* 2012;2:1223-1237.
7. Papademetriou IT, Porter T. Promising approaches to circumvent the blood-brain barrier: Progress, pitfalls and clinical prospects in brain cancer. *Ther Deliv* 2015;6:989-1016.
8. Drean A, Lemaire N, Bouchoux G, et al. Temporary blood-brain barrier disruption by low intensity pulsed ultrasound increases carboplatin delivery and efficacy in preclinical models of glioblastoma. *J Neurooncol* 2019;144:33-41.
9. Liu HL, Huang CY, Chen JY, Wang HY, Chen PY, Wei KC. Pharmacodynamic and therapeutic investigation of focused ultrasound-induced blood-brain barrier opening for enhanced temozolomide delivery in glioma treatment. *PLOS One* 2014;9:e114311.
10. Kovacs Z, Werner B, Rassi A, Sass JO, Martin-Fiori E, Bernasconi M. Prolonged survival upon ultrasound-enhanced doxorubicin delivery in two syngenic glioblastoma mouse models. *J Control Release* 2014; 187:74-82.
11. Coluccia D, Figueiredo CA, Wu MY, et al. Enhancing glioblastoma treatment using cisplatin-gold-nanoparticle conjugates and targeted delivery with magnetic resonance-guided focused ultrasound. *Nano-medicine* 2018;14:1137-1148.
12. Zhang DY, Dmello C, Chen L, et al. Ultrasound-mediated delivery of paclitaxel for glioma: A comparative study of distribution, toxicity, and efficacy of albumin-bound versus cremophor formulations. *Clin Cancer Res* 2020;26:477-486.
13. Beccaria K, Canney M, Bouchoux G, et al. Ultrasound-induced blood-brain barrier disruption for the treatment of gliomas and other primary CNS tumors. *Cancer Lett* 2020;479:13-22.
14. Non-invasive Blood-brain Barrier Opening in Alzheimer's Disease Patients Using Focused Ultrasound. NLM identifier: NCT04118764 Available from: <https://www.clinicaltrials.gov/ct2/show/NCT04118764> Accessed May 3, 2020.
15. Blood-Brain Barrier Opening Using MR-Guided Focused Ultrasound in Patients With Amyotrophic Lateral Sclerosis. NLM identifier: NCT03321487. Available at: <https://www.clinicaltrials.gov/ct2/show/NCT03321487>. Accessed May 3, 2020.
16. Stupp R, Mason WP, van den Bent MJ, et al. Radiotherapy plus concomitant and adjuvant temozolomide for glioblastoma. *N Engl J Med* 2005;352:987-996.
17. Koshy M, Villano JL, Dolecek TA, et al. Improved survival time trends for glioblastoma using the SEER 17 population-based registries. *J Neurooncol* 2012;107:207-212.
18. Ostrom QT, Cioffi G, Gittleman H, et al. CBTRUS statistical report: Primary brain and other central nervous system tumors diagnosed in the United States in 2012–2016. *Neuro Oncol* 2019;21(suppl 5): v1-v100.
19. Oberoi RK, Parrish KE, Sio TT, Mittapalli RK, Elmquist WF, Sarkaria JN. Strategies to improve delivery of anticancer drugs across the blood-brain barrier to treat glioblastoma. *Neuro-oncology* 2016;18: 27-36.
20. Sarkaria JN, Hu LS, Parney IF, et al. Is the blood-brain barrier really disrupted in all glioblastomas? A critical assessment of existing clinical data. *Neuro Oncol* 2018;20:184-191.
21. Hande KR. Etoposide: Four decades of development of a topoisomerase II inhibitor. *Eur J Cancer* 1998;34:1514-1521.
22. Mehta A, Awah CU, Sonabend AM. Topoisomerase II poisons for glioblastoma: Existing challenges and opportunities to personalize therapy. *Front Neurol* 2018;9:459.
23. Franceschi E, Cavallo G, Scopece L, et al. Phase II trial of carboplatin and etoposide for patients with recurrent high-grade glioma. *Br J Cancer* 2004;91:1038-1044.
24. Reardon DA, Desjardins A, Vredenburgh JJ, et al. Metronomic chemotherapy with daily, oral etoposide plus bevacizumab for recurrent malignant glioma: A phase II study. *Br J Cancer* 2009;101:1986-1994.
25. Aoki T, Mizutani T, Nojima K, et al. Phase II study of ifosfamide, carboplatin, and etoposide in patients with a first recurrence of glioblastoma multiforme. *J Neurosurg* 2010;112:50-56.
26. Kesari S, Schiff D, Doherty L, et al. Phase II study of metronomic chemotherapy for recurrent malignant gliomas in adults. *Neuro Oncol* 2007;9:354-363.
27. Liu B, Earl HM, Poole CJ, Dunn J, Kerr DJ. Etoposide protein binding in cancer patients. *Cancer Chemother Pharmacol* 1995;36:506-512.
28. Sonabend AM, Yun J, Lei L, et al. Murine cell line model of proneural glioma for evaluation of anti-tumor therapies. *J Neurooncol* 2013;112: 375-382.
29. Pouliopoulos AN, Jimenez DA, Frank A, et al. Temporal stability of lipid-shelled microbubbles during acoustically-mediated blood-brain barrier opening. Original research. *Front Physics* 2020;8:137.
30. Pouliopoulos AN, Burgess MT, Konofagou EE. Pulse inversion enhances the passive mapping of microbubble-based ultrasound therapy. *Appl Phys Lett* 2018;113:044102.
31. Pouliopoulos AN, Bonaccorsi S, Choi JJ. Exploiting flow to control the in vitro spatiotemporal distribution of microbubble-seeded acoustic cavitation activity in ultrasound therapy. *Phys Med Biol* 2014;59:6941-6957.
32. Pouliopoulos AN, Wu SY, Burgess MT, Karakatsani ME, Kamimura HAS, Konofagou EE. A clinical system for non-invasive blood-brain barrier opening using a neuronavigation-guided single-element focused ultrasound transducer. *Ultrasound Med Biol* 2020;46: 73-89.
33. Villanueva-Meyer JE, Mabray MC, Cha S. Current clinical brain tumor imaging. *Neurosurgery* 2017;81:397-415.
34. Gaspar LE, Fisher BJ, Macdonald DR, et al. Supratentorial malignant glioma: Patterns of recurrence and implications for external beam local treatment. *Int J Radiat Oncol Biol Phys* 1992;24:55-57.
35. Lee SW, Fraass BA, Marsh LH, et al. Patterns of failure following high-dose 3-D conformal radiotherapy for high-grade astrocytomas: A quantitative dosimetric study. *Int J Radiat Oncol Biol Phys* 1999;43: 79-88.
36. Jacobs VL, Valdes PA, Hickey WF, De Leo JA. Current review of in vivo GBM rodent models: Emphasis on the CNS-1 tumour model. *ASN Neuro* 2011;3:e00063.
37. Radaelli E, Ceruti R, Patton V, et al. Immunohistopathological and neuroimaging characterization of murine orthotopic xenograft models of glioblastoma multiforme recapitulating the most salient features of human disease. *Histol Histopathol* 2009;24:879-891.
38. Bond AE, Shah BB, Huss DS, et al. Safety and efficacy of focused ultrasound thalamotomy for patients with medication-refractory, tremor-dominant Parkinson disease: A randomized clinical trial. *JAMA Neurol* 2017;74:1412-1418.
39. Bunevicius A, McDannold NJ, Golby AJ. Focused ultrasound strategies for brain tumor therapy. *Oper Neurosurg (Hagerstown)* 2020;19: 9-18.
40. Lipsman N, Meng Y, Bethune AJ, et al. Blood-brain barrier opening in Alzheimer's disease using MR-guided focused ultrasound. *Nat Commun* 2018;9:2336.
41. Idbaih A, Canney M, Belin L, et al. Safety and feasibility of repeated and transient blood-brain barrier disruption by pulsed ultrasound in patients with recurrent glioblastoma. *Clin Cancer Res* 2019;25:3793-3801.
42. Asquier N, Bouchoux G, Canney M, et al. Blood-brain barrier disruption in humans using an implantable ultrasound device: Quantification with MR images and correlation with local acoustic pressure. *J Neurosurg* 2019;1-9.
43. Abraham A, Meng Y, Llinas M, et al. First-in-human trial of blood-brain barrier opening in amyotrophic lateral sclerosis using MR-guided focused ultrasound. *Nat Commun* 2019;10:4373.
44. Kinoshita M, McDannold N, Jolesz FA, Hynynen K. Noninvasive localized delivery of Herceptin to the mouse brain by MRI-guided

- focused ultrasound-induced blood-brain barrier disruption. *Proc Natl Acad Sci USA* 2006;103:11719-11723.
45. Liu HL, Hsu PH, Lin CY, et al. Focused ultrasound enhances central nervous system delivery of bevacizumab for malignant glioma treatment. *Radiology* 2016;281:99-108.
 46. Kobus T, Zervantonakis IK, Zhang Y, McDannold NJ. Growth inhibition in a brain metastasis model by antibody delivery using focused ultrasound-mediated blood-brain barrier disruption. *J Control Release* 2016;238:281-288.
 47. Park EJ, Zhang YZ, Vykhodtseva N, McDannold N. Ultrasound-mediated blood-brain/blood-tumor barrier disruption improves outcomes with trastuzumab in a breast cancer brain metastasis model. *J Control Release* 2012;163:277-284.
 48. Hande K, Messenger M, Wagner J, Krozely M, Kaul S. Inter- and inpatient variability in etoposide kinetics with oral and intravenous drug administration. *Clin Cancer Res* 1999;5:2742-2747.
 49. Sonabend AM, Carminucci AS, Amendolara B, et al. Convection-enhanced delivery of etoposide is effective against murine proneural glioblastoma. *Neuro Oncol* 2014;16:1210-1219.
 50. Leonard A, Wolff JE. Etoposide improves survival in high-grade glioma: A meta-analysis. *Anticancer Res* 2013;33:3307-3315.